J. Fluid Mech. (1989), *vol.* 202, *pp.* 499–514
Printed in Great Britain

Divided discharges for divided flows

By RONALD SMITH
Department of Applied Mathematics and Theoretical Physics, University of Cambridge, Silver Street, Cambridge CB3 9EW, UK

(Received 12 February 1988 and in revised form 21 June 1988)

An effluent outlet within thirty channel breadths upstream of a branching in a river can lead to high shoreline pollution levels along one of the branches, or near the tip of the central region. This paper identifies an optimal splitting of a steady discharge that minimizes the shoreline pollution.

1. Introduction

For a single steady outlet within thirty channel breadths upstream of a river delta, it is not possible to avoid relatively high shoreline pollution levels. Depending upon whereabouts across the flow the outlet is sited, either the contaminant plume will impinge on the tip of the central region, or the bulk of the contaminant will enter just one of the branches (giving comparatively high shoreline pollution levels further downstream in that branch).

The ideal discharge strategy would be to make the discharge rate at each point across the river proportional to the local river volume flow rate. This would ensure that the concentration immediately was uniform across the flow. So, no matter how the flow branched, there could be no regions of anomalously high shoreline concentrations. Alas, the practicalities of avoiding interference with other river uses, and maintaining the discharge from silting or damage, makes this ideal untenable. If a single outlet is environmentally unacceptable, then the next best engineering solution would be two outlets.

If the discharge is divided (see figure 1), then it should be possible to position the outlets so that neither of the two plumes impinge on the tip of the branching. Also, by adjusting the relative strengths of the discharges, it may be possible to avoid high shoreline concentrations along either of the branches. The present paper gives a constructive procedure for determining the optimal positions and strengths. It is shown that the improvements as regards shoreline concentrations can be quite considerable.

Divided discharges and divided flows have received attention from Daish (1985*a*, *b*), but in the context of sudden discharges. For steady discharges, the mirror-image situation of merging tributaries has been studied by the author (Smith 1988). Except in the basic principles, there is no substantial mathematical overlap.

2. Advection-diffusion equation

As shown by Yotsukura & Cobb (1972) and by Yotsukura & Sayre (1976), the use of flow-following coordinates virtually eliminates all the geometrical complications of meandering streams. Thus, for the main calculations we shall ignore longitudinal variations. The modifications needed to cope with meandering are pointed out in the Appendix.

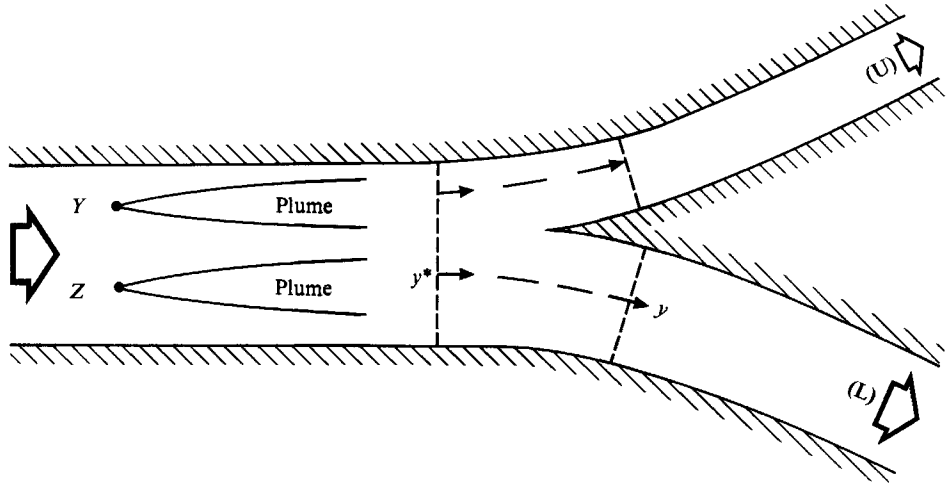

FIGURE 1. Sketch of a river delta with a divided discharge so that the pollution load is shared between the two downstream branches. In practice the plumes would be very much narrower and much further upstream.

The x-direction is along the flow, with $x = 0$ defining the position where the river splits into two branches. The y-direction is across the flow, with the shoreline positions denoted by y_-, y_+. It is unduly restrictive to enforce flow-following matching of y across the branching. So, proper account will need to be made for the matching of an upstream flow line y^* to a downstream flow line y (see figure 1).

For rivers with depth $h(y)$ much less than the breadth, the appropriate depth-averaged advection–diffusion equation is

$$hu\,\partial_x c = \partial_y(h\kappa\,\partial_y c). \tag{2.1a}$$

Here $u(y)$ is the depth-averaged longitudinal velocity, $c(x, y)$ is the concentration, and $\kappa(y)$ is the effective transverse diffusivity. At the shorelines the no-flux boundary condition is

$$h\kappa\,\partial_y c = 0 \quad \text{on} \quad y = y_-, y_+. \tag{2.1b}$$

Diffusion along the flow can be neglected by virtue of the fact that contaminant plumes in rivers are extremely long and narrow (i.e. the downstream e-folding distance for cross-sectional mixing is about 30 times the total channel breadth).

3. Eigenmodes

A separation of variables solution of (2.1a, b) leads to the introduction of the eigenmodes $\phi_n(y)$:

$$\frac{\mathrm{d}}{\mathrm{d}y}\left(h\kappa\frac{\mathrm{d}\phi_n}{\mathrm{d}y}\right) + \mu_n hu\phi_n = 0, \tag{3.1a}$$

with

$$h\kappa\frac{\mathrm{d}\phi_n}{\mathrm{d}y} = 0 \quad \text{on} \quad y = y_-, y_+, \tag{3.1b}$$

$$\int_{y_-}^{y_+} hu\phi_n^2\,\mathrm{d}y = \int_{y_-}^{y_+} hu\,\mathrm{d}y = Q. \tag{3.1c}$$

Q is the volume flow rate for this stretch of the river system. The zero mode is

$$\phi_0 = 1, \quad \mu_0 = 0 \tag{3.2a, b}$$

The eigenvalues μ_n increase with n. The nth eigenmode ϕ_n has n zeros across the flow, and the zeros of successive eigenmodes interlace. In particular, ϕ_1 has opposite signs at the two shorelines.

The solution for $c(x, y)$ can be represented:

$$c = c_0 + \sum_{n=1}^{\infty} c_n \exp(-\mu_n x)\, \phi_n(y). \tag{3.3}$$

If the concentration profile were known at some cross-section, say $x = 0$, then the weight factors c_n can be evaluated:

$$c_n = \frac{1}{Q} \int_{y_-}^{y_+} hu \phi_n c \, dy. \tag{3.4}$$

Far downstream, the approach to uniformity is dominated by the first non-zero coefficient $c_1, c_2, \ldots$. This led Smith (1982) to deduce that the only way to avoid concentrations in excess of c_0 at either of the river banks is to require that

$$c_1 = 0. \tag{3.5}$$

This could be achieved by a single plume sited at the zero of the first mode ϕ_1.

Here, with two rivers downstream of the flow division, we have to ensure that there is no overshoot in either the upper or lower branch:

$$c_1^{(U)} = c_1^{(L)} = 0 \tag{3.6a, b}$$

Also, we have to divide the pollution load between the branches so that the eventual shoreline concentrations in each branch are the same:

$$c_0^{(U)} = c_0^{(L)}. \tag{3.6c}$$

The longitudinal lengthscale over which cross-sectional mixing takes place is sufficiently long that in a river delta there could be multiple branchings. The necessary generalization of (3.6*a*–*c*) would be to require that c_1 be zero and c_0 should share the common value in all of the eventual branches.

4. Upstream extrapolation

Our objective is to relate the downstream constraints (3.6*a*–*c*) upon the concentration to the upstream condition at the divided discharge. To do this, we use the reciprocity properties of the advection–diffusion equation (F. B. Smith 1957).

Across the relatively short flow-adjustment region, we use flow-following to define upstream functions $\Phi_1^{(U)}, \Phi_1^{(L)}, \Psi$:

for y in upper branch

$$\Phi_1^{(U)}(0, y^*) = \phi_1^{(U)}(y), \tag{4.1a}$$

$$\Phi_1^{(L)}(0, y^*) = 0, \tag{4.1b}$$

$$\Psi(0, y^*) = Q^{(L)}/Q^*; \tag{4.1c}$$

for y in lower branch

$$\Phi_1^{(U)}(0, y^*) = 0, \tag{4.2a}$$

$$\Phi_1^{(L)}(0, y^*) = \phi_1^{(L)}(y), \tag{4.2b}$$

$$\Psi(0, y^*) = -Q^{(U)}/Q^*. \tag{4.2c}$$

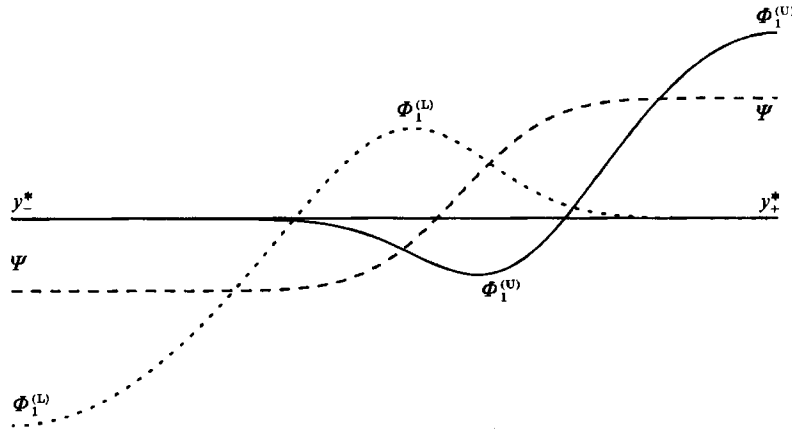

FIGURE 2. Cross-stream profiles of the functions $\Phi^{(U)}$ (——), $\Phi^{(L)}$ (· · · ·), and Φ (– – –), at a moderate distance upstream of a branching. (The illustrative example in §8 is used with parameter values $x = -\frac{1}{4}L^*, s = \frac{1}{4}$.)

Here y^* denotes the position upstream of the branching that links to the downstream position y (see figure 1). The superscripts $*$, (U), (L) are used to distinguish quantities associated with the original channel and the two branches (Daish 1985*b*).

In terms of the upstream concentration, depth and velocity profiles, the conditions (3.6*a–c*) for the avoidance of excessive shoreline pollution become

$$\int_{y_-^*}^{y_+^*} hu\Phi_1^{(U)}\, c\, \mathrm{d}y^* = \int_{y_-^*}^{y_+^*} hu\Phi_1^{(L)}\, c\, \mathrm{d}y^* = 0, \tag{4.3a, b}$$

$$\int_{y_-^*}^{y_+^*} hu\Psi c\, \mathrm{d}y^* = 0 \quad \text{at} \quad x = 0. \tag{4.3c}$$

If we are to apply these conditions at some other value of x (e.g. at the divided discharge), then we need to define appropriate upstream extrapolations for $\Phi_1^{(U)}, \Phi_1^{(L)}, \Psi$. The work of F. B. Smith (1957) reveals that since $c(x, y^*)$ is a solution of the advection–diffusion equation (2.1*a, b*), then $\Phi_1^{(U)}, \Phi_1^{(L)}, \Psi$ should all be solutions of the adjoint (reversed-flow) equation

$$-hu\,\partial_x \Psi = \partial_y(hK\,\partial_y \Psi), \tag{4.4a}$$

with

$$hK\,\partial_y \Psi = 0 \quad \text{on} \quad y = y_-^*, y_+^*. \tag{4.4b}$$

It then follows that ∂_x of each of the integrals (4.3*a–c*) is zero. At moderate distances upstream of the branching the cross-stream profiles of $\Phi_1^{(U)}, \Phi_1^{(L)}, \Psi$ can be expected to have the relative shapes sketched in figure 2. We emphasize that $\Phi_1^{(U)}, \Phi_1^{(L)}, \Psi$ are *not* eigenmodes of the upstream reach.

For a branching network there would be additional Φ- and Ψ-functions. Moreover, there would have to be repeated flow-following matching to extend the functions upstream to where the divided discharge is to be made.

5. Dividing the discharge

Such is the disparity (1:30) between the total breadth of a river and the downstream e-folding for transverse mixing, that for a divided discharge we can ignore the longitudinal separation. At a fixed longitudinal position x_0 the two

discharge positions are denoted by $y^* = Y, y^* = Z$. Thus, the concentration is approximated by a pair of delta functions

$$huc = q[\alpha\delta(y^*-Y)+\beta\delta(y^*-Z)], \tag{5.1a}$$

with

$$\alpha+\beta = 1, \tag{5.1b}$$

where q is the total discharge strength. In general, the number of separate plumes would correspond to the number of river branches. For the division $\alpha q, \beta q$ of the discharge strength to be physically realizable, it is necessary that α and β both be positive.

Substituting for *huc* into the upstream extrapolation of the conditions (4.3*a–c*) we arrive at the equations

$$\alpha\Phi_1^{(U)}(Y)+\beta\Phi_1^{(U)}(Z) = 0, \tag{5.2a}$$

$$\alpha\Phi_1^{(L)}(Y)+\beta\Phi_1^{(L)}(Z) = 0, \tag{5.2b}$$

$$\alpha\Psi(Y)+\beta\Psi(Z) = 0. \tag{5.2c}$$

For clarity the dependence upon x_0 has been suppressed; it is the same for $\Phi_1^{(U)}$, $\Phi_1^{(L)}$, and Ψ. The three functions $\Phi_1^{(U)}$, $\Phi_1^{(L)}$, Ψ can be regarded as being known. Our task is to find α, β, Y, Z.

If we assume that the zeros of the three functions are in the order $\Phi_1^{(L)}$, Ψ, $\Phi_1^{(U)}$ (as shown in figure 2), then it is convenient to use the Ψ-equation (5.2*c*) to eliminate α, β. Each of the remaining equations (5.2*a*, *b*) can then be interpreted as defining the zero contours in the (Y, Z)-plane of the antisymmetric combinations

$$\frac{\Phi_1^{(U)}(Y)}{\Psi(Y)}-\frac{\Phi_1^{(U)}(Z)}{\Psi(Z)}, \quad \frac{\Phi_1^{(L)}(Y)}{\Psi(Y)}-\frac{\Phi_1^{(L)}(Z)}{\Psi(Z)}. \tag{5.3a, b}$$

Close to the branching we can infer that these contours have the relative shapes sketched in figure 3. Without loss of generality we can restrict attention to Z less than, and Y greater than, the zero of Ψ.

Figure 4 gives a sketch of the quotients $\Phi_1^{(U)}/\Psi$ and $\Phi_1^{(L)}/\Psi$. For a given value of Z (to the left of the singularity), we can evaluate the $^{(U)}$ and $^{(L)}$ quotients. The right-hand side positions where these respective quotients have the same values are denoted $Y^{(U)}(Z), Y^{(L)}(Z)$. Likewise for a given value of Y (to the right of the singularity) we can associate $Z^{(U)}(Y), Z^{(L)}(Y)$. These are alternative ways of representing the zero contours of the combinations (5.3*a*, *b*):

$$(Y^{(U)}(Z), Z), \quad (Y^{(L)}(Z), Z) \quad \text{or} \quad (Y, Z^{(U)}(Y)), \quad (Y, Z^{(L)}(Y)). \tag{5.4}$$

A sufficient condition for there to be an intersection of the zero contours is that their ordering is different along the two boundaries $Z = y_-^*, Y = y_+^*$. For example, this would be ensured if

$$Y^{(L)}(y_-^*) < Y^{(U)}(y_-^*) \quad \text{and} \quad Z^{(L)}(y_+^*) < Z^{(U)}(y_+^*) \tag{5.5}$$

(see figure 3). The same topological considerations reveal as x_0 varies that the intersection could only be lost through the boundary (i.e. when one of the optimal positions is at one of the shorelines). Similarly, multiple intersections would have to originate from the shorelines. We shall assume that the solution for (Y, Z) is unique.

If we have an approximation (Y_n, Z_n) to the optimal discharge pairing, then we

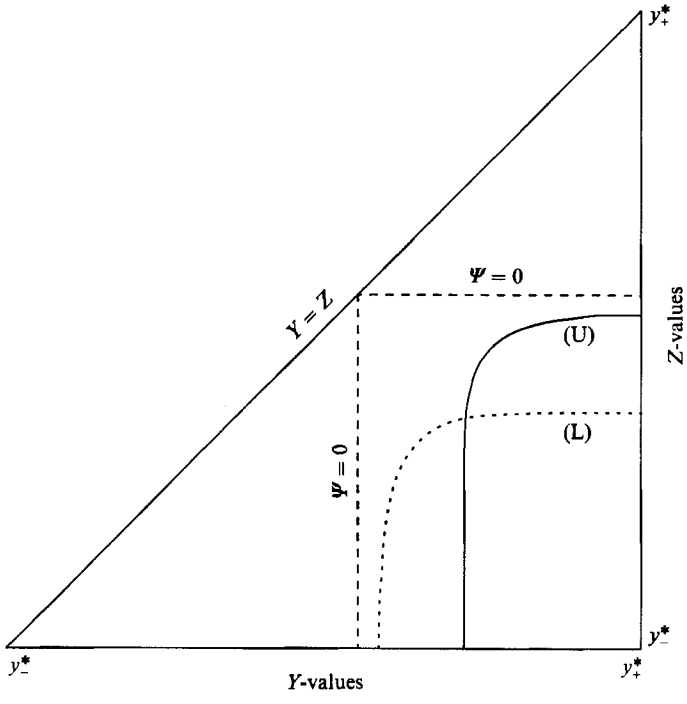

FIGURE 3. Zero contours of the antisymmetric combinations defined in (5.3a, b) for varied pairs of discharge sites (Y, Z). The intersection defines the optimal pair of discharge sites at a given distance upstream of the branching. (Again, the illustrative example in §8 has been used with the parameter values $x = -\frac{1}{4}L^*, s = \frac{1}{4}$.)

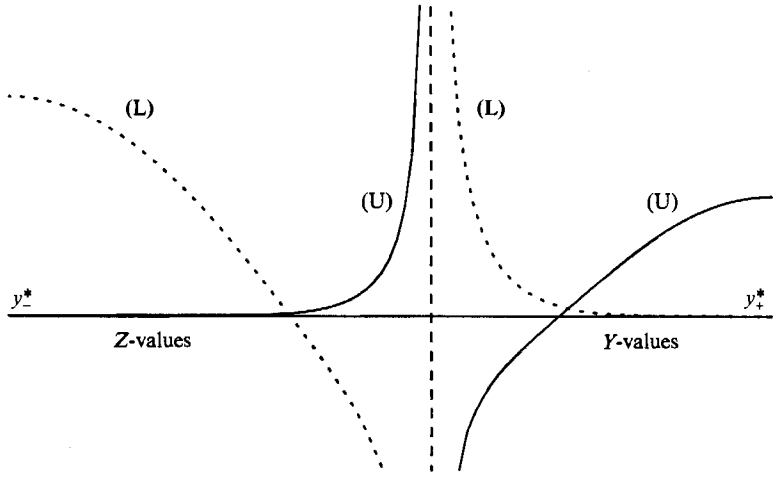

FIGURE 4. Cross-stream profiles of the quotients $\Phi^{(U)}/\Psi$ (——), and $\Phi^{(L)}/\Psi$ (· · ·), at a moderate distance upstream of a branching (Once more, the illustrative example in §8 has been used with the parameter values $x = -\frac{1}{4}L^*, s = \frac{1}{4}$.)

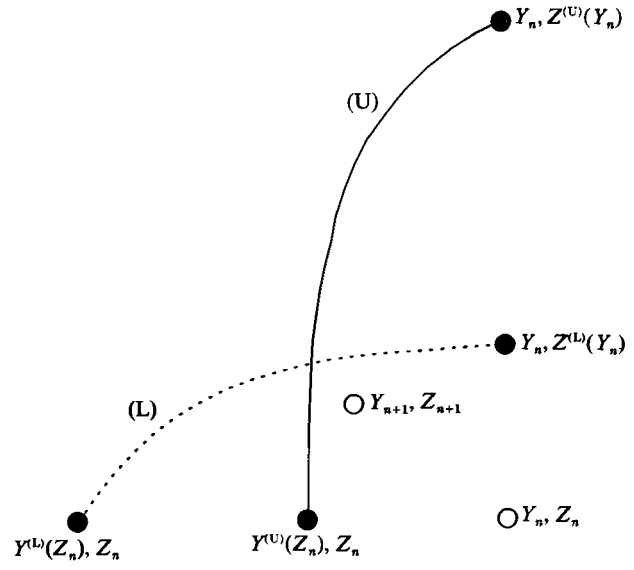

FIGURE 5. Definition sketch of the subsidiary points (shaded circles) used to construct successive approximations (open circles) to the optimal division of the discharge.

can use the quotient graphs to generate points that lie on the zero contours (see figure 5):

$$(Y_n, Z^{(U)}(Y_n)), \quad (Y^{(U)}(Z_n), Z_n), \quad (Y_n, Z^{(L)}(Y_n)), \quad (Y^{(L)}(Z_n), Z_n). \qquad (5.6a\text{–}d)$$

The intersection of the chords from the $^{(U)}$ and $^{(L)}$ points gives a much improved estimate of the optimal discharge pairing

$$Y_{n+1} = Y_n - (Y_n - Y^{(U)}(Z_n))\,(Y_n - Y^{(L)}(Z_n))\,(Z^{(U)}(Y_n) - Z^{(L)}(Y_n))/\Delta, \qquad (5.7a)$$

$$Z_{n+1} = Z_n + (Z^{(U)}(Y_n) - Z_n)\,(Z^{(L)}(Y_n) - Z_n)\,(Y^{(U)}(Z_n) - Y^{(L)}(Z_n))/\Delta, \qquad (5.7b)$$

with

$$\Delta = (Y_n - Y^{(L)}(Z_n))\,(Z^{(U)}(Y_n) - Z_n) - (Y_n - Y^{(U)}(Z_n))\,(Z^{(L)}(Y_n) - Z_n). \qquad (5.7c)$$

This gives a rapidly convergent constructive procedure to compute Y, Z.

Once the optimal positions (Y, Z) have been determined, the corresponding division α, β of the discharge strength is given by

$$\alpha = \frac{-\Psi(Z)}{\Psi(Y) - \Psi(Z)}, \quad \beta = \frac{\Psi(Y)}{\Psi(Y) - \Psi(Z)}. \qquad (5.8a, b)$$

Since Y and Z are at opposite sides of the single zero of Ψ, it necessarily follows that α and β are positive, i.e. that the division $\alpha q, \beta q$ of the discharge strength is physically realizable.

6. Discharges close to and far from the branching

If the divided discharge is only just upstream of the branching, then, from (4.1*b*), (4.2*a*) it follows that, for any Y, Z in the respective parts of the flow we have

$$\Phi_1^{(L)}(Y) = 0, \quad \Phi_1^{(U)}(Z) = 0. \qquad (6.1a, b)$$

Hence, (5.2a, b) force us to choose Y, Z to correspond (via flow-following) to the zeros of the downstream modes

$$\phi_1^{(U)}(y) = 0, \quad \phi_1^{(L)}(z) = 0. \tag{6.2a, b}$$

These are precisely the optimal discharge positions for a single point discharge in each of the branches (Smith 1982). Moreover, the piecewise-constant values of Ψ (4.1c, 4.2c) ensure that the division (5.8a, b) of the discharge strengths is in the ratio of the volume flow rates for the two branches:

$$\alpha = Q^{(U)}/Q^*, \quad \beta = Q^{(L)}/Q^*. \tag{6.3a, b}$$

To investigate optimal discharges far upstream of the branching, we pose the representations

$$\Phi_1^{(U)} = \sum_{n=1}^{\infty} p_n^{(U)} \exp(\mu_n^* x)\, \phi_n^*(y^*), \tag{6.4a}$$

$$\Phi_1^{(L)} = \sum_{n=1}^{\infty} p_n^{(L)} \exp(\mu_n^* x)\, \phi_n^*(y^*), \tag{6.4b}$$

$$\Psi = \sum_{n=1}^{\infty} r_n \exp(\mu_n^* x)\, \phi_n^*(y^*). \tag{6.4c}$$

The asterisks indicate that these are upstream modes and eigenvalues. The initial conditions (4.1), (4.2) guarantee the absence of any $n = 0$ components, and ensure that $p_1^{(U)}, p_1^{(L)}, r_1$ are non-zero.

The zero contours in the (Y, Z)-plane defined by (5.3a, b) are equivalent to the pair of equations

$$0 = \sum_{n=1}^{\infty} \sum_{m=1}^{\infty} p_n^{(U)} r_m \exp[(\mu_n^* + \mu_m) x_0]\, [\phi_n^*(Y)\, \phi_m^*(Z) - \phi_n^*(Z)\, \phi_m^*(Y)], \tag{6.5a}$$

$$0 = \sum_{n=1}^{\infty} \sum_{m=1}^{\infty} p_n^{(L)} r_m \exp[(\mu_n^* + \mu_m) x_0]\, [\phi_n^*(Y)\, \phi_m^*(Z) - \phi_n^*(Z)\, \phi_m^*(Y)]. \tag{6.5b}$$

We note that the $n = m$ terms have zero coefficients.

At large distances upstream of the branching, the optimal sites Y, Z become independent of x_0 (or the coefficients $p_n^{(U)}, p_n^{(L)}, r_n$) and satisfy the pair of equations

$$0 = \phi_1^*(Y)\, \phi_2^*(Z) - \phi_1^*(Z)\, \phi_2^*(Y), \quad 0 = \phi_1^*(Y)\, \phi_3^*(Z) - \phi_1^*(Z)\, \phi_3^*(Y). \tag{6.6a, b}$$

Figure 6 shows the zero contours in the (X, Y)-plane associated with these ϕ_2^* and ϕ_3^* equations. The intersection defines the asymptotic optimal sites. It deserves emphasis that there is no dependence upon the distance from, nor nature $(Q^{(U)}, Q^{(L)})$ of the branching.

In (6.5a, b) the departure from the asymptote (6.6a, b) is dominated by the $(\mu_2^* + \mu_3^*)$ term. Hence, we can infer that the convergence of (Y, Z) to the upstream asymptote is at the fast rate $\exp[(\mu_3^* - \mu_1^*) x_0]$. The corresponding longitudinal e-folding length is about 18 times the river breadth.

Far upstream, the formulae (5.8a, b) for the discharge strength becomes

$$\alpha = \frac{-\phi_1^*(Z)}{\phi_1^*(Y) - \phi_1^*(Z)}, \quad \beta = \frac{\phi_1^*(Y)}{\phi_1^*(Y) - \phi_1^*(Z)}. \tag{6.7a, b}$$

By virtue of the results (6.6a, b), we can replace ϕ_1^* by either ϕ_2^* or ϕ_3^*.

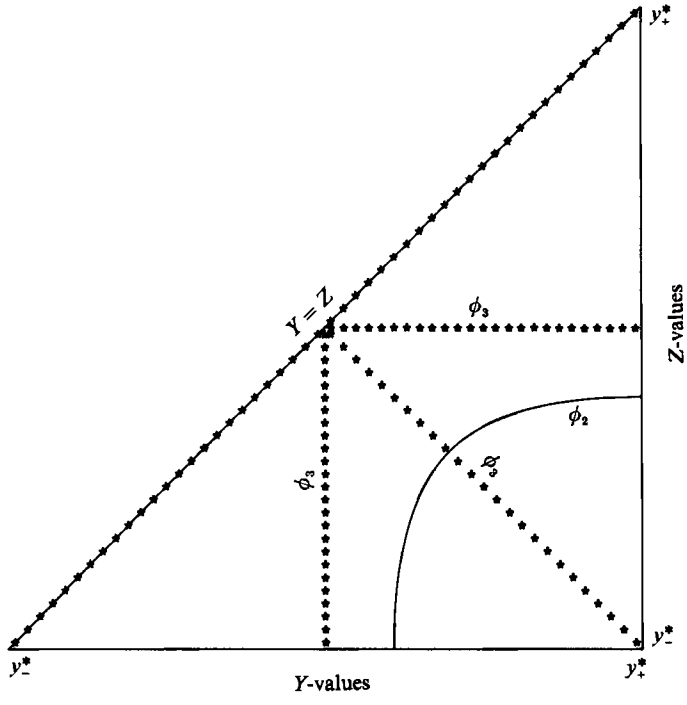

FIGURE 6. Zero contours of the antisymmetric combinations (6.5), (6.6) involving the ϕ_2 mode (——), and the ϕ_3 mode (stars). The intersection defines the asymptotic pair of discharge sites (Y, Z) far upstream of the branching.

Upstream of the branching an appropriate representation for the concentration $c(x, y^*)$ would be

$$c = c_0^* + \sum_{n=1}^{\infty} c_n^* \exp\left[-\mu_n^*(x-x_0)\right]\phi_n^*(y^*). \tag{6.8}$$

For the double delta-function discharge (5.1a), the weight factors c_n^* are given by

$$c_n^* = q[\alpha\phi_n^*(Y) + \beta\phi_n^*(Z)]. \tag{6.9}$$

If we use the formulae (6.7a, b), we can deduce that when the discharge position x_0 is far upstream, then

$$c_1^* = c_2^* = c_3^* = 0. \tag{6.10}$$

Hence, the departure from uniformity is dominated by the fourth mode ϕ_4^*, and the approach to uniformity is at the fast rate $\exp\left[-\mu_4^*(x-x_0)\right]$. The corresponding e-folding length is about nine channel breadths. It is this rapid approach to uniformity that permits the same optimal discharge specification Y, Z, α, β to apply to *any* subsequent flow division.

7. Avoiding local pollution

The separate plumes can be thought of as going into the respective branches (see figure 1). So, in view of the work of Smith (1982), we can anticipate that there will not be any local regions of high shoreline concentration. However, in the absence of a proof, it is sensible to take the precaution of investigating the possibility of locally unacceptable pollution.

To evaluate the concentration at the tip we introduce a Green function $G(x, y)$ corresponding to a delta-function discharge at the tip in the reversed flow:

$$-hu\,\partial_x G - \partial_y (h\kappa\,\partial_y G) = Q\delta(x)\delta(y^* - y_{\text{tip}}), \tag{7.1a}$$

with

$$h\kappa\,\partial_y G = 0 \quad \text{on} \quad y^* = y^*_-, y^*_+. \tag{7.1b}$$

The much used reciprocity properties of the advection–diffusion equation (F. B. Smith 1957), enable us to evaluate the tip concentration in terms of the discharge conditions:

$$c_{\text{tip}} = q[\alpha G(x, Y) + \beta G(x, Z)]. \tag{7.2}$$

Hence, to avoid unacceptable pollution at the tip we require

$$\alpha G(x, Y) + \beta G(x, Z) \leqslant 1. \tag{7.3}$$

In terms of the upstream eigenmodes ϕ^*_n, the Green function has the representation

$$G = 1 + \sum_{n=1}^{\infty} \exp(\mu^*_n x)\,\phi^*_n(y_{\text{tip}})\,\phi^*_n(y^*). \tag{7.4}$$

Strictly, the conditions (3.6a–c) merely ensure that in both branches the approach to the asymptotic concentration c_0 is in the same sense at the two sides of each channel. Smith (1982) checked the nature of the approach by evaluating the next coefficient c_2 in the representation (3.3). Thus, by analogy with $\Phi^{(\mathrm{U})}_1, \Phi^{(\mathrm{L})}_1$ we also define upstream extensions $\Phi^{(\mathrm{U})}_2, \Phi^{(\mathrm{L})}_2$ of the second modes:

for y in upper branch

$$\Phi^{(\mathrm{U})}_2(0, y^*) = \phi^{(\mathrm{U})}_2(y), \tag{7.5a}$$

$$\Phi^{(\mathrm{L})}_2(0, y^*) = 0, \tag{7.5b}$$

for y in lower branch

$$\Phi^{(\mathrm{U})}_2(0, y^*) = 0, \tag{7.6a}$$

$$\Phi^{(\mathrm{L})}_2(0, y^*) = \phi^{(\mathrm{L})}_2(y). \tag{7.6b}$$

As before, y^* denotes the cross-stream position upstream of the branching that links to the downstream position y (see figure 1). Without loss of generality we select the signs of the modes $\phi^{(\mathrm{U})}_2, \phi^{(\mathrm{L})}_2$ so that they are positive at the shorelines.

At the branching the $c^{(\mathrm{U})}_2, c^{(\mathrm{L})}_2$ coefficients (3.4) can be evaluated in terms of the upstream concentration, depth and velocity profiles:

$$c^{(\mathrm{U})}_2 = \frac{1}{Q^{(\mathrm{U})}} \int_{y_-}^{y_+} hu\Phi^{(\mathrm{U})}_2\, c\,\mathrm{d}y^* \quad \text{at} \quad x = 0, \tag{7.7a}$$

$$c^{(\mathrm{L})}_2 = \frac{1}{Q^{(\mathrm{L})}} \int_{y_-}^{y_+} hu\Phi^{(\mathrm{L})}_2\, c\,\mathrm{d}y^* \quad \text{at} \quad x = 0. \tag{7.7b}$$

With the sign convention that $\phi^{(\mathrm{U})}_2, \phi^{(\mathrm{L})}_2$ are positive at the shorelines, the condition for no overshoot of concentration at the shorelines is that

$$c^{(\mathrm{U})}_2 < 0, \quad c^{(\mathrm{L})}_2 < 0. \tag{7.8a, b}$$

Provided that $\Phi^{(\mathrm{U})}_2, \Phi^{(\mathrm{L})}_2$ satisfy the reversed-flow equation (4.4a, b), then the integrals (7.7a, b) remain constant for x upstream of the branching (F. B. Smith 1957). In particular, at the divided discharge the delta-function structure (5.1a) of huc, yields the requirements

$$\alpha\Phi^{(\mathrm{U})}_2(Y) + \beta\Phi^{(\mathrm{U})}_2(Z) < 0, \quad \alpha\Phi^{(\mathrm{L})}_2(Y) + \beta\Phi^{(\mathrm{L})}_2(Z) < 0. \tag{7.9a, b}$$

Thus, once a provisional optimization has been obtained by the constructive scheme (5.7), (5.8), we use these requirements (7.3), (7.9*a*, *b*) to test the acceptability of the specification $(x_0, Y, Z, \alpha, \beta)$. The numerical evidence of the special case studied in the next section is that the optimization is always acceptable.

8. Illustrative example

A simple example which permits explicit solutions for $\Phi_1^{(U)}, \Phi_1^{(L)}, \Psi, \Phi_2^{(U)}, \Phi_2^{(L)}$ is when the depth, velocity and diffusivity are proportional to each other:

$$h = H[\cos(\pi y/2B)]^{\frac{1}{2}}, \quad u = U[\cos(\pi y/2B)]^{\frac{1}{2}}, \tag{8.1a, b}$$

$$\kappa = K[\cos(\pi y/2B)]^{\frac{1}{2}}, \tag{8.1c}$$

with

$$y_- = -B, \quad y_+ = B, \quad Q = 4HUB/\pi. \tag{8.1d–f}$$

The eigenmodes are Legendre polynomials:

$$\phi_n = (2n+1)^{\frac{1}{2}} P_n(\eta), \tag{8.2a}$$

$$\mu_n = \frac{n(n+1)\pi^2 K}{4UB^2}, \quad \eta = \sin\frac{\pi y}{2B}. \tag{8.2b, c}$$

We introduce a parameter s which indicates the splitting of the river volume flux Q^* between the upper and lower branches:

$$Q^{(U)} = \tfrac{1}{2}(1-s)Q^*, \quad Q^{(L)} = \tfrac{1}{2}(1+s)Q^*. \tag{8.3a, b}$$

The flow-following matching across the junction gives

$$Q^*[1-\eta^*] = Q^{(U)}[1-\eta] \quad \text{for } y \text{ in upper branch}, \tag{8.4a}$$

$$Q^*[1+\eta^*] = Q^{(L)}[1+\eta] \quad \text{for } y \text{ in lower branch}, \tag{8.4b}$$

$$\eta = \frac{1}{1-s}(2\eta^* - 1 + s) \quad \text{for} \quad \eta^* > s, \tag{8.4c}$$

$$\eta = \frac{1}{1+s}(2\eta^* + 1 - s) \quad \text{for} \quad \eta^* < s. \tag{8.4d}$$

Hence, just upstream of the branching the starting values for the required functions are (first for $\eta^* > s$)

$$(\tfrac{1}{3})^{\frac{1}{2}}\Phi_1^{(U)} = \frac{1}{1-s}(2\eta^* - (1+s)) \tag{8.5a}$$

$$(\tfrac{1}{3})^{\frac{1}{2}}\Phi_1^{(L)} = 0, \quad \Psi = \tfrac{1}{2}(1+s), \tag{8.5b, c}$$

$$(\tfrac{1}{5})^{\frac{1}{2}}\Phi_2^{(U)} = \frac{1}{(1-s)^2}(6\eta^{*2} - 6(1+s)\eta^* + 1 + 4s + s^2), \quad (\tfrac{1}{5})^{\frac{1}{2}}\Phi_2^{(L)} = 0; \tag{8.5d, e}$$

(and secondly for $\eta^* < s$)

$$(\tfrac{1}{3})^{\frac{1}{2}}\Phi_1^{(U)} = 0, \quad (\tfrac{1}{3})^{\frac{1}{2}}\Phi_1^{(L)} = \frac{1}{1+s}(2\eta^* + 1 - s), \tag{8.6a, b}$$

$$\Psi = -\tfrac{1}{2}(1-s), \quad (\tfrac{1}{5})^{\frac{1}{2}}\Phi_2^{(U)} = 0, \tag{8.6d}$$

$$(\tfrac{1}{5})^{\frac{1}{2}}\Phi_2^{(L)} = \frac{1}{(1+s)^2}(6\eta^{*2} + 6(1-s)\eta^* + 1 - 4s + s^2). \tag{8.6e}$$

Legendre series for these same starting conditions at $x = 0$ are

$$(\tfrac{1}{3})^{\frac{1}{2}}\Phi_1^{(\mathrm{U})} = \tfrac{1}{4}(1-s)^2\eta^* + \frac{1}{1-s}\sum_{n=2}^{\infty} \times (\tfrac{1}{2}(1+3s)\,[P_{n+1}(s)-P_{n-1}(s)]+P_{n-2}(s)-P_{n+2}(s))\,P_n(\eta^*), \quad (8.7a)$$

$$(\tfrac{1}{3})^{\frac{1}{2}}\Phi_1^{(\mathrm{L})} = \tfrac{1}{4}(1+s)^2\eta^* + \frac{1}{1+s}\sum_{n=2}^{\infty} \times (\tfrac{1}{2}(1-3s)\,[P_{n+1}(s)-P_{n-1}(s)]+P_{n+2}(s)-P_{n-2}(s))\,P_n(\eta^*), \quad (8.7b)$$

$$\Psi = \sum_{n=1}^{\infty} \tfrac{1}{2}[P_{n-1}(s)-P_{n+1}(s)]\,P_n(\eta^*), \quad (8.7c)$$

$$\begin{aligned}(\tfrac{1}{5})^{\frac{1}{2}}\Phi_2^{(\mathrm{U})} = {} & \tfrac{1}{8}(1-s)^3(\tfrac{3}{2}\eta^{*2}-\tfrac{1}{2}) \\ & + \frac{1}{(1-s)^2}\sum_{n=3}^{\infty}(\tfrac{1}{2}(1+10s+13s^2)\,[P_{n-1}(s)-P_{n+1}(s)] \\ & - 3(1+2s)\,[P_{n-2}(s)-P_{n+2}(s)] + \frac{3(n+1)}{2n+3}\,[P_{n-1}(s)-P_{n+3}(s)] \\ & + \frac{3n}{2n-1}\,[P_{n-3}(s)-P_{n+1}(s)])\,P_n(\eta^*), \end{aligned} \quad (8.7d)$$

$$\begin{aligned}(\tfrac{1}{5})^{\frac{1}{2}}\Phi_2^{(\mathrm{L})} = {} & \tfrac{1}{8}(1+s)^3(\tfrac{3}{2}\eta^{*2}-\tfrac{1}{2}) \\ & - \frac{1}{(1+s)^2}\sum_{n=3}^{\infty}(\tfrac{1}{2}(1-10s+13s^2)\,[P_{n-1}(s)-P_{n+1}(s)] \\ & + 3(1-2s)\,[P_{n-2}(s)-P_{n+2}(s)] + \frac{3(n+1)}{2n+3}\,[P_{n-1}(s)-P_{n+3}(s)] \\ & + \frac{3n}{2n-1}\,[P_{n-3}(s)-P_{n+1}(s)])\,P_n(\eta^*). \end{aligned} \quad (8.7e)$$

To obtain the Legendre series solutions further upstream, we simply need multiply the coefficient of $P_n(\eta^*)$ by the appropriate exponential factor

$$\exp\left(\frac{n(n+1)\,\pi^2K^*x}{4U^*B^{*2}}\right). \quad (8.8)$$

From the $n = 2$ mode we can define a typical longitudinal lengthscale L^* for transverse mixing:

$$L^* = \frac{2u^*B^{*2}}{3\pi^2K^*}. \quad (8.9)$$

Typically L^* corresonds to a longitudinal distance of about $60B^*$ or thirty channel breadths (Smith 1988, equation (6.11)). The illustrative figures 2–5 are based upon the special case

$$s = \tfrac{1}{4}, \quad x = -\tfrac{1}{4}L^* \quad (8.10a, b)$$

(i.e. the flow divides in the ratio 3:5 at a distance of about $15B^*$ downstream of the divided discharge). For a river of total breadth 100 m this would be an outlet 750 m upstream of the branching.

Figure 7(*a*) shows the optimal discharge positions Y, Z as functions of the upstream distance x for fixed (positive) values of s (i.e. when the larger fraction $\frac{1}{2}(1+s)Q^*$ of the total river flow Q^* goes into the lower branch). For negative s the results need to be inverted vertically. The acceptability tests (7.3), (7.8*a*, *b*) are

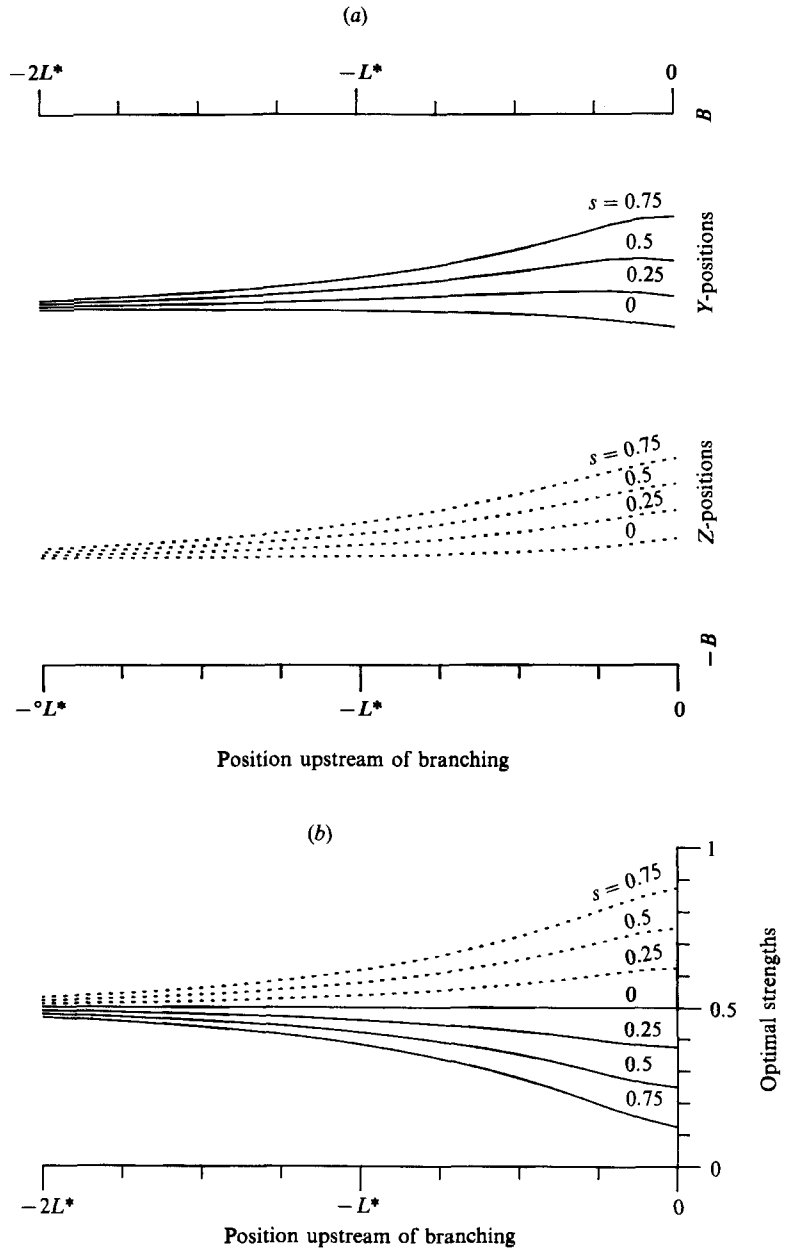

FIGURE 7. (*a*) Optimal pairs of discharge positions ——, · · · · for fixed partitions $\frac{1}{2}(1-s):\frac{1}{2}(1+s)$ of the river volume flow between the upper and lower branches. The diffusion lengthscale L^* typically corresponds to about thirty times the total width of the channel. (*b*) Optimal pairs of discharge strengths ——, · · · for the divided discharge positions as given in (*a*).

satisfied at all the points calculated. Figure 7(*b*) shows the optimal discharge strengths. In keeping with the general predictions made in §6, both figures 7(*a*) and 7(*b*) exhibit rapid approaches to the upstream asymptote

$$Y = -Z = \frac{2B^*}{\pi}\arcsin\left(\frac{1}{\sqrt{3}}\right) = 0.392B^*, \quad \alpha = \beta = \tfrac{1}{2}. \qquad (8.11a, b)$$

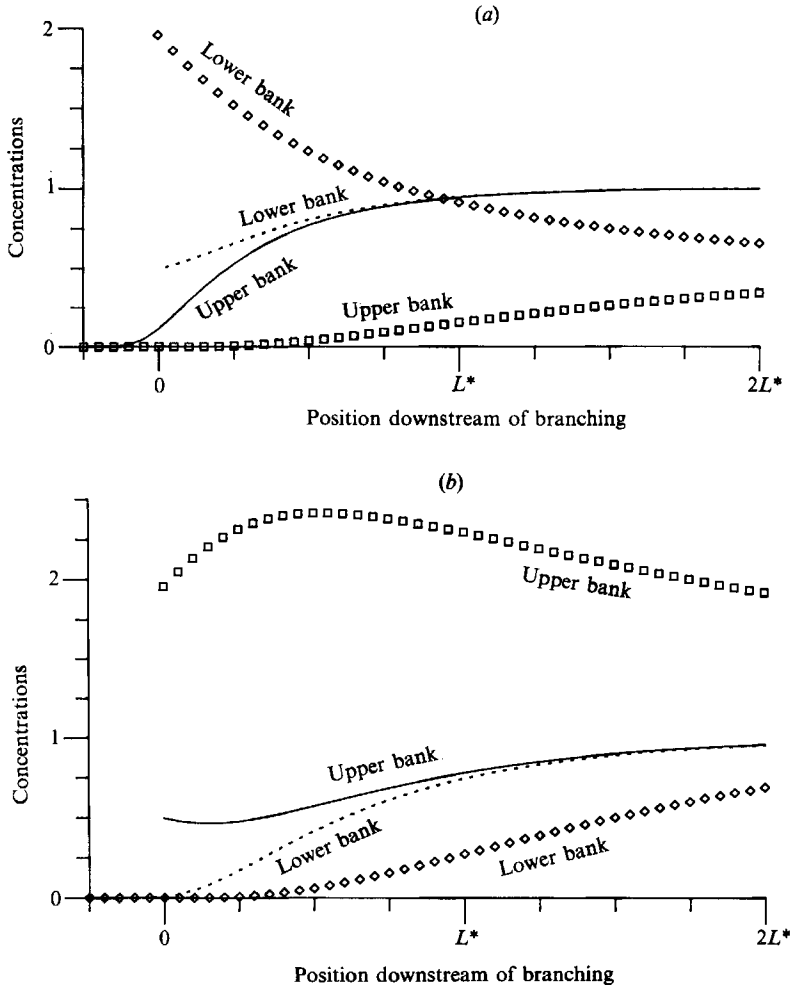

FIGURE 8. Shoreline concentrations along (*a*) the smaller (upper) river branch and (*b*) the larger (lower) river branch. ——, · · · correspond to the optimal divided discharge; the open diamonds and squares correspond to a single centreline discharge (which but for the branching would itself be optimal).

Figure 8(*a*, *b*) illustrates the difference in shoreline concentrations for single and divided discharges. The discharge takes place at a distance $\frac{1}{4}L^*$ upstream of the branching with asymmetry parameter $s = \frac{1}{4}$. The single discharge is at the centreline. (To fix the downstream lengthscales we have assumed that the mixing lengths for the branches scale as the respective volume discharge rates $Q^{(U)}, Q^{(L)}$). For a river of total breadth 100 m, the discharge would be 0.75 km upstream of the branching and the results shown in figure 8(*a*, *b*) extend to a downstream distance of 6 km. Prior to the branching the single centreline discharge minimizes the shoreline concentration. It is downstream of the branching that the shortcomings of the single discharge become apparent. Figure 8(*a*) shows that for the upper branch there are anomalously high concentrations near the tip, while figure 8(*b*) shows that for the wider lower branch there are high concentrations even at large distances (because more than $\frac{5}{8}$ of the contaminant load enters that branch). By contrast, the divided discharge achieves

its objective of keeping the concentrations along all four shorelines below the lowest possible upper bound.

The financial support of the Royal Society is gratefully acknowledged.

Appendix. Varying streams

For clarity the above analysis precluded any x-dependence of the flow properties. This Appendix details the minor changes that are needed to contend with this additional complication.

To avoid the need for more than one velocity component, we align the coordinates x and y along and across the streamlines. The non-uniformity with respect to x implies that the distance increments m_1, m_2 in the two coordinate directions are functions of position x, y. Thus the advection–diffusion equation (2.1a) takes the form

$$m_2 hu\,\partial_x c = \partial_y[(m_1/m_2)\,h\kappa\,\partial_y c], \tag{A 1a}$$

with

$$\partial_x(m_2 hu) = 0. \tag{A 1b}$$

The counterpart of the separation-of-variables representation (3.3), (3.4) is

$$c = c_0 + \sum_{n=1}^{\infty} c_n \exp\left(-\int_0^x \mu_n(x')\,m_1\,\mathrm{d}x'\right)\phi_n(x,y), \tag{A 2a}$$

with

$$c_n = \frac{1}{Q}\int_{y_-}^{y_+} m_2 hu\hat{\phi}_n\, c\,\mathrm{d}y \quad \text{at} \quad x = 0 \tag{A 2b}$$

(Smith 1982). The co- and counterflow modes $\phi_n, \hat{\phi}_n$ satisfy the adjoint equations

$$m_2 hu\,\partial_x \phi_n = \partial_y[(m_1/m_2)\,h\kappa\,\partial_y \phi_n] + \mu_n m_1 m_2 hu\phi_n, \tag{A 3a}$$

$$-m_2 hu\,\partial_x \hat{\phi}_n = \partial_y[(m_1/m_2)\,h\kappa\,\partial_y \hat{\phi}_n] + \mu_n m_1 m_2 hu\hat{\phi}_n, \tag{A 3b}$$

$$h\kappa\,\partial_y \phi_n = h\kappa\,\partial_y \hat{\phi}_n = 0 \quad \text{on} \quad y = y_+, y_-, \tag{A 3c}$$

$$\int_{y_-}^{y_+} m_2 hu\phi_n \hat{\phi}_n\,\mathrm{d}y = Q, \tag{A 3d}$$

$$\int_{y_-}^{y_+} m_2 hu\phi_n\,\partial_x \hat{\phi}_n\,\mathrm{d}y = \int_{y_-}^{y_+} m_2 hu\hat{\phi}_n\,\partial_x \phi_n\,\mathrm{d}y = 0, \tag{A 3e}$$

$$\phi_n = \hat{\phi}_n \quad \text{at the branching} \quad x = 0. \tag{A 3f}$$

As before, the condition for no concentration overshoot is that

$$c_1 = 0. \tag{A 4}$$

Since the definition of c_1 involves the counterflow mode $\hat{\phi}_1$, the upstream extension $\hat{\Phi}_1$ must match to this same mode:

$$\hat{\Phi}_1 = \hat{\phi}_1 \quad \text{at} \quad x = 0.$$

Except for this occurrence of the counterflow mode $\hat{\phi}_1$ in the definition of $\hat{\Phi}_1$, the analysis proceeds exactly as in the uniform case.

REFERENCES

DAISH, N. C. 1985*a* Optimal discharge profiles for sudden contaminant releases in steady uniform open-channel flow. *J. Fluid Mech.* **159**, 303–321.

DAISH, N. C. 1985*b* Shear dispersion problems in open-channel flows. Ph.D. thesis, University of Cambridge, 128 pp.

SMITH, F. B. 1957 The diffusion of smoke from a continuous elevated point source into a turbulent atmosphere. *J. Fluid Mech.* **2**, 49–76.

SMITH, R. 1982 Where to put a steady discharge in a river. *J. Fluid Mech.* **115**, 1–11.

SMITH, R. 1988 Minimizing shoreline pollution in rivers with tributaries. *J. Fluid Mech.* **187**, 589–597.

YOTSUKURA, N. & COBB, E. D. 1972 Transverse diffusion of solutions in natural stream. *US Geo. Survey Paper* 582-C.

YOTSUKURA, N. & SAYRE, W. W. 1976 Transverse mixing in natural channels. *Wat. Resour. Res.* **12**, 695–704.